



TECHNICAL UNIVERSITY OF CLUJ-NAPOCA

ACTA TECHNICA NAPOCENSIS

Series: Applied Mathematics, Mechanics, and Engineering  
Vol. 67, Issue I, March, 2024

## MODELING AND SIMULATION OF AN ULTRASONIC CONCENTRATOR USED IN A FEED SYSTEM FOR ULTRASONICALLY AIDED MICROEDM

Bogdan-Ionuț CRISTEA, Liviu Daniel GHICULESCU, Aurel Mihail TITU,  
Constantin-Cristian DEOPALE

**Abstract:** This study presents a numerical modeling approach to optimize an ultrasonic concentrator for micro electrical discharge machining (microEDM) applications at a target frequency of 40805 Hz. The concentrator's dimensions and shape are adjusted through an optimization process to achieve a high amplification coefficient. A nodal channel is incorporated to mark the region where the amplification is minimum. The resulting concentrator has a frequency of 40557 Hz and an amplification coefficient of 2.71. The concentrator and transducer are connected using an 18 mm long M12 bolt. Testing validates the model, which results in an eigenfrequency of 40696 Hz, which is subsequently machined to reach the target frequency. The study demonstrates a valuable method for designing and optimizing concentrators for specific frequency applications.

**Key words:** micro electrical discharge machining, ultrasonic concentrator, feed system, transducer, eigenfrequency

### 1. INTRODUCTION

Electrical discharge machining (EDM) is a material removal process that uses electric discharges between two electrodes (workpiece and tool) in a dielectric fluid [1]. Non-stationary electric discharges, or sparks, occur between the electrodes, resulting in the removal of material. The sparks occur sequentially, separated from each other. The space between the electrode tool and the workpiece is called the spark gap. The size of the spark gap varies and is dependent on voltage, amperage, electrode materials, and type of dielectric used. Higher voltage and amperage lead to a larger spark gap, facilitating material removal.

Regular cleaning of the spark gap is crucial for maintaining a stable EDM process and preventing short-circuits [2]. Accumulated debris can disrupt the process' stability and have adverse effects on the surface quality of both tool and workpiece.

Micro electrical discharge machining (microEDM) is a scaled-down version of EDM, involving miniature and more delicate electrode

tools. This introduces limitations in terms of flushing techniques and imposes restrictions on amperage and voltage values in order to prevent excessive tool wear [3]. Consequently, a very small volume of material is removed. However, the trade-off is a higher quality surface finish [4], making it popular for micro-level surface finishing in various industries [5].

To overcome the low productivity and frequent short-circuits of microEDM, researchers have explored ultrasonically aided micro electrical discharge machining [6].

In this technique, ultrasonic vibrations are utilized to enhance spark gap flushing and improve surface finishing. The oscillating movement of the electrode induced by ultrasonic vibrations generates a pumping effect within the spark gap. This mechanism effectively propels the expelled material outward [6].

Subsequent research expanded on microEDM+US:

1. RTDUV (Relative Three-Dimensional Ultrasonic Vibration) was used to improve debris removal performance. Overall machining efficiency was enhanced by 19.5% [7];

2. A high-frequency ultrasonic vibration system was designed as a solution to improve the efficiency of microEDM. It enhanced the process' efficiency by 82.7% [8].

3. Sensor based discharge data acquisition and response measurements revealed that vibration assistance of microEDM is beneficial, resulting in an 18% increase in discharge energy and a reduction in surface roughness of 0.45  $\mu\text{m}$ , down from 3.2  $\mu\text{m}$  on high-energy settings [9].

4. UCV (Ultrasonic Circular Vibration) electrode was used to improve microhole machining performances. Results showed that the electrode had a lower retreat frequency and that debris adhesions was reduced on the inner wall of the microhole. The increased relative velocity between electrode and workpiece also reduced abnormal discharges and led to a more stable machining process [10].

5. A rotary tool electrode was used to machine Inconel 718, an extremely difficult to machine material using conventional processes. The study found out that productivity increased with high ultrasonic power, and most importantly on high tool RPM [11].

MicroEDM+US employs an ultrasonic chain which is composed of a transducer and a concentrator (horn). The transducer converts electrical energy, received from the US generator, into mechanical oscillation energy with ultrasonic frequency. The horn amplifies and concentrates the vibration amplitude (transmitted by the transducer) at the end of the ultrasonic chain.

For optimal operation, the resonance condition must be achieved between the transducer and concentrator. This requires matching the eigenfrequency of the transducer, which represents the target frequency provided by the manufacturer of ultrasonic transducers – Institute of Solid Mechanics of the Romanian Academy (IMSAR), and the eigenfrequency of the concentrator which integrates the tool electrode.

This study focuses on the modelling and optimization of an ultrasonic concentrator to achieve a high amplification coefficient and a target eigenfrequency of 40805 Hz, as specified by the transducer manufacturer (IMSAR).

The designed ultrasonic concentrator finds application in the field of ultrasonically aided

micro electrical discharge machining, particularly in industries requiring high precision surface finishing for micro-components.

## 2. SETUP

The process begins with a simple step concentrator, which is then optimized to achieve a high amplification coefficient (K) and a target eigenfrequency ( $f_{cr}$ ) of 40805 Hz, in close proximity to the transducer's eigenfrequency ( $f_{tr}$ ). The transducer's parameters are presented in table 1, and the initial parameters of the concentrator are listed in table 2.

Table 1

Transducer parameters	
Parameter	Value
Transducer eigenfrequency $f_{tr}$	40805 Hz
Radiant bushing diameter $D_{br}$	35 mm
Radiant bushing thread	M12x1.75

Table 2

Initial concentrator parameters	
Parameter	Value
Material	Steel AISI 4340
Young's elasticity modulus E	$2.1 * 10^{11}$ Pa
Material density $\rho$	7850 Kg/m <sup>3</sup>

The material properties of AISI 4340, used for the concentrator, are displayed in table 3.

Table 3

Material properties of AISI 4340	
Parameter	Value
Code	Steel AISI 4340
Density [Kg/m <sup>3</sup> ]	7850
Young's Modulus [Pa]	$2.1 * 10^{11}$
Poisson Coefficient [-]	0.28

## 3. INITIAL STEP

The initial concentrator, which serves as the starting point for the research paper, is modelled through the following steps:

**Step 1.** Calculation of the wavelength ( $\lambda$ )

The wavelength ( $\lambda$ ) is given using formula 1:

$$\lambda = \frac{c}{f} = \frac{1}{f} * \sqrt{\frac{E}{\rho}} \text{ [m]} \quad (1)$$

where: c – speed of sound in the concentrator material [m/s]; f – frequency [Hz], where an

arbitrary value of 37000 is selected to ensure that the designed concentrator doesn't overshoot the target eigenfrequency;  $E$  – Young's Modulus [Pa];  $\rho$  – material density [ $\text{Kg/m}^3$ ].

Replacing in relation 1, the following result is obtained:

$$\lambda = \frac{1}{37\,000} * \sqrt{\frac{2.1 * 10^{11}}{7\,850}} \Rightarrow \lambda = 0.1397 \text{ m}$$

**Step 2.** Calculation of the wavenumber ( $\alpha$ )

The wavenumber ( $\alpha$ ) is calculated using formula 2, which relates the wavelength and the frequency.

$$\lambda\alpha = \frac{2 * \pi}{\lambda} [m^{-1}] \quad (2)$$

Replacing in relation 2, the following result is obtained:

$$\alpha = \frac{2 * \pi}{0.1397} \Rightarrow \alpha = 44.9476 \text{ m}^{-1}$$

**Step 3.** Initial lengths determination

The 2 lengths of the step concentrator are determined using relations 3 and 4, based on the work of Merkulov and Kharitonov [12]:

$$l_1 = \frac{1,5}{\alpha} [m] \quad (3)$$

$$l_2 = \frac{1,6}{\alpha} [m] \quad (4)$$

Replacing in relations 3 and 4, the 2 lengths of the concentrator are obtained:

$$l_1 = \frac{1,5}{44.9476} \Rightarrow l_1 = 33.372 \text{ mm}$$

$$l_2 = \frac{1,6}{44.9476} \Rightarrow l_2 = 35.596 \text{ mm}$$

**Step 4.** Initial diameters values

The first diameter of the step concentrator is chosen to match the diameter of the transducer ( $D = D_{tr} = 35 \text{ mm}$ ). The second diameter is chosen constructively with a value of  $d = 20 \text{ mm}$ .

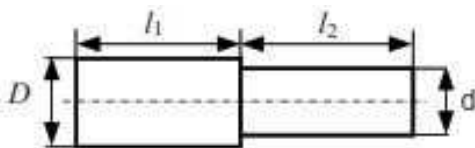


**Fig. 1.** Shape and dimensions of a step concentrator

Figure 1 illustrates the shape and dimensions of the starting step concentrator.

These steps outline the process of modelling the initial concentrator and provide the necessary

parameters and dimensions for further analysis and optimization in the research paper.

## 4. MODELING OF THE CONCENTRATOR

The ultrasonic concentrator is modelled and designed using Comsol Multiphysics finite element software, employing the Structural Mechanics module and the Eigenfrequency study for precise analysis.

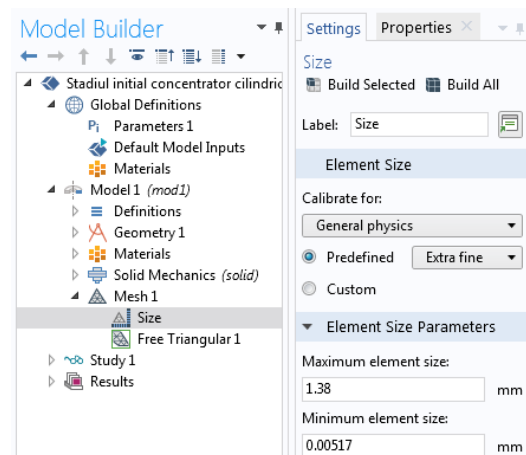
The concentrator is made of steel AISI 4340, and the electrode from 99.5% copper. The geometry of the concentrator is constructed in a 2D axisymmetric space using the initial parameters outlined in table 4. All parameters are introduced in Comsol to model the concentrator.

Table 4

Parameters for the initial step of the concentrator

Name	Expression	Value	Description
l1	33.372 [mm]	0.033372 m	upper step length
r1	17.5 [mm]	0.0175 m	upper step radius
l2	35.596 [mm]	0.035596 m	lower step length
r2	10 [mm]	0.01 m	lower step radius
rr	r1 – r2	0.0075 m	radius between steps
modulE	2.1E11	2.1E11	Young's Modulus

The element size is calibrated for an extra fine level (figure 2), resulting in an average quality of elements of 0.9256 on a scale from 0 to 1 (figure 3).



**Fig. 2.** Mesh settings

Complete mesh	
Mesh vertices:	729
Element type:	All elements
Triangles:	1331
Edge elements:	125
Vertex elements:	7
— Domain element statistics —	
Number of elements:	1331
Minimum element quality:	0.6782
Average element quality:	0.9256
Element area ratio:	0.2717
Mesh area:	952.3 mm <sup>2</sup>

Fig. 3. Mesh statistics for initial step of the concentrator

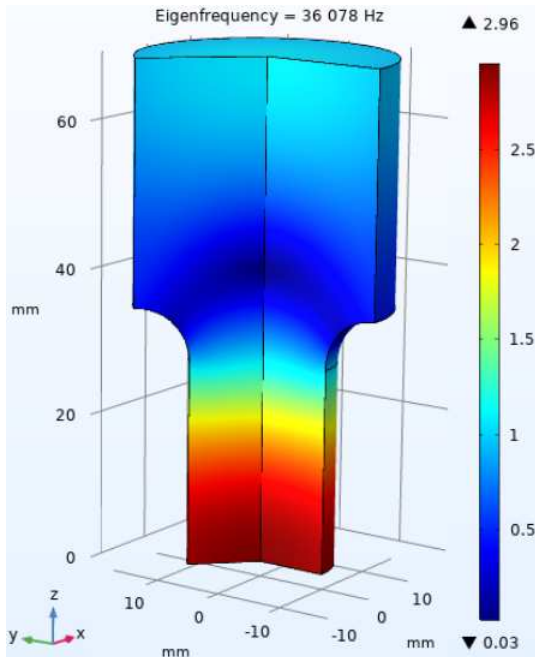


Fig. 4. Eigenfrequency and amplification for the initial step of the concentrator

In figure 4 the concentrator's eigenfrequency  $f_{cr} = 36078$  Hz and amplification factor  $K = 2.96$  are displayed.

To reach the target frequency of 40805 Hz, from the initial eigenfrequency of 36078 Hz, a number of adjustment steps are made. Each step modifies the geometry of the concentrator, and implicitly its eigenfrequency and amplification coefficient.

**Step 1 & 2.** Add an inclination angle to the lower step of the concentrator

An inclination angle ( $\alpha$ ) of  $1^\circ$  is added to the lower step of the concentrator. The parameters for step 1 are presented in table 5.

Table 5

Parameters for step 1 of the concentrator

Name	Expression	Value	Description
l1	33.372 [mm]	0.033372 m	upper step length
r1	17.5 [mm]	0.0175 m	upper step radius
l2	35.596 [mm]	0.035596 m	lower step length
r2	10 [mm]	0.01 m	lower step radius
rr	$r1 - r2$	0.0075 m	radius between steps
module	2.1E11	2.1E11	Young's Modulus
alfa	1 [°]	1°	inclination angle

Figure 5 shows that adding an inclination angle ( $\alpha$ ) of  $1^\circ$  slightly increased the number of elements from 1331 to 1332 and reduced the average element quality to 0.9138.

Complete mesh	
Mesh vertices:	729
Element type:	All elements
Triangles:	1332
Edge elements:	124
Vertex elements:	8
— Domain element statistics —	
Number of elements:	1332
Minimum element quality:	0.628
Average element quality:	0.9138
Element area ratio:	0.2308
Mesh area:	946.8 mm <sup>2</sup>

Fig. 5. Mesh statistics for step 1 concentrator at inclination angle  $\alpha = 1^\circ$

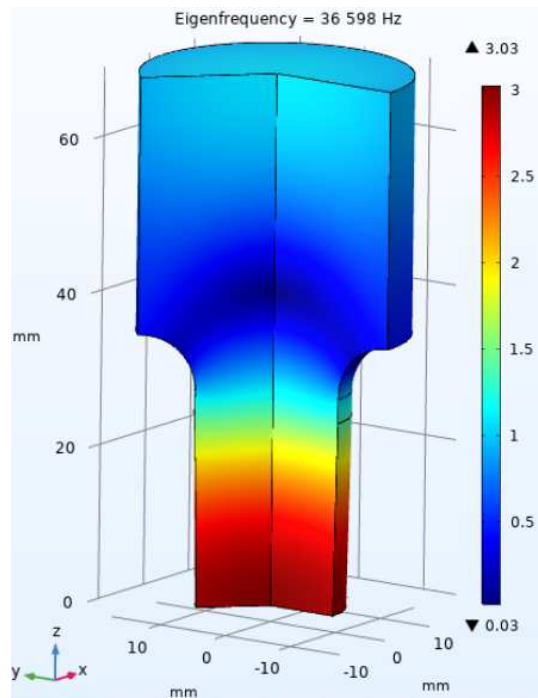


Fig. 6. Eigenfrequency and amplification in step 1 of the concentrator ( $\alpha = 1^\circ$ )

In comparison to the initial step, step 1 has an increase in amplification from 2.96 to 3.03, and an increase in eigenfrequency from 36078 Hz to 36598 Hz. In order to see the effects of the inclination angle has on the concentrator, table 6 is created. Where the frontal surface of the concentrator is added, which will be used to model the filiform electrode in later steps.

Table 6

**Inclination angle variation and effects on ultrasonic parameters**

Angle [°]	Eigenfrequency [Hz]	Amplification coefficient [-]	Frontal surface [mm <sup>2</sup> ]
1	36 598	3.03	19.12
2	37 136	3.05	18.25
3	37 693	3.07	17.38
4	38 271	3.14	16.5
5	38 870	3.15	15.62
6	39 491	3.17	14.74
7	40 134	3.23	13.86
8	40 800	3.25	12.96
9	41 489	3.27	12.08
<b>10</b>	<b>42 202</b>	<b>3.34</b>	<b>11.18</b>
11	42 936	3.35	10.28
12	43 690	3.39	9.36
13	44 463	3.44	8.44
14	45 249	3.46	7.54
15	46 044	3.48	6.6

An increase in angle leads to an increase in eigenfrequency and amplification coefficient and a decrease in the frontal surface. Since this surface will be used to assemble the filiform electrode, a value of 10° is chosen, leaving enough surface available for the electrode's housing and the welding required to keep it in place. The inclination angle of 10° decreased the number of elements decreased to 1278 and slightly reduced the element quality to 0.9119 (figure 7).

**Complete mesh**

Mesh vertices:	701
Element type:	All elements
Triangles:	1278
Edge elements:	122
Vertex elements:	8
— Domain element statistics —	
Number of elements:	1278
Minimum element quality:	0.628
Average element quality:	0.9119
Element area ratio:	0.2273
Mesh area:	897.2 mm <sup>2</sup>

**Fig. 7.** Mesh statistics for step 2 concentrator at inclination angle of  $\alpha = 10^\circ$

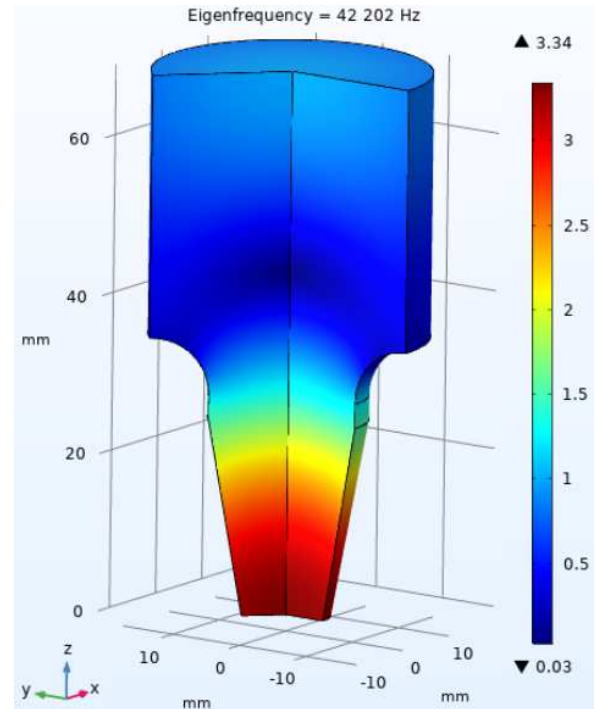


**Fig. 8.** Eigenfrequency and amplification in step 2 of the concentrator ( $\alpha = 10^\circ$ )

From figure 6 and figure 8, it can be observed that increasing the inclination angle to  $\alpha = 10^\circ$  leads to an increase in eigenfrequency, from 36598 Hz to 42202 Hz. And an increase in the amplification factor from 3.03 to 3.34.

**Step 3.** Add the filiform electrode

The filiform electrode (made of 99.5% pure Cu) and its housing are added to the concentrator. The following parameters (table 7) are added: hole radius = 0.2 mm, hole depth = 5 mm, the length of the electrode = 15 mm, Young's modulus for copper and silver and finally the height of the weld = 3.5 mm.

Table 7

**Parameters for step 3 of the concentrator**

Name	Expression	Value	Description
l1	33.372 [mm]	0.033372 m	upper step length
r1	17.5 [mm]	0.0175 m	upper step radius
l2	35.596 [mm]	0.035596 m	lower step length
r2	10 [mm]	0.01 m	lower step radius
rr	$r1 - r2$	0.0075 m	radius between steps
modulE	2.1E11	2.1E11	Young's Modulus
alfa	1 [°]	1°	inclination angle
rgaurasc	0.2 [mm]	2E-4 m	wire hole radius
hgaurasc	5 [mm]	0.005 m	wire hole depth
lscula	15 [mm]	0.015 m	electrode length

modulE Cu	130 [GPa]	1.3E11 Pa	Young's Modulus for copper
hlipire	3.5 [mm]	0.0035 m	weld height
modulE Ag	69 [GPa]	6.9E10 Pa	Young's Modulus for silver

The number of elements increased to 1565 and the quality decreased to 0.87 as presented in figure 9. The addition of the filiform electrode, including Ag welding, led to a decrease in eigenfrequency to 41425 Hz and a decrease in amplification to 2.37 (figure 10).

**Complete mesh**

Mesh vertices: 882

Element type: **All elements**

Triangles: 1565

Edge elements: 237

Vertex elements: 13

— Domain element statistics —

Number of elements: 1565

Minimum element quality: 0.5498

Average element quality: 0.8747

Element area ratio: 0.007702

Mesh area: 908.7 mm<sup>2</sup>

Fig. 9. Mesh statistics for step 3 concentrator

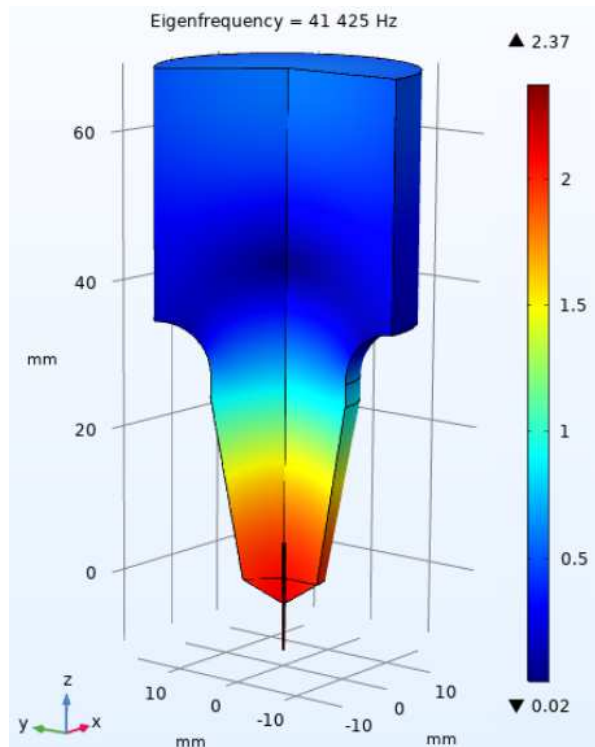


Fig. 10. Eigenfrequency and amplification in step 3 of the concentrator

**Step 4. Add a threaded hole for stud assembly**

A threaded hole is added for the assembly of the ultrasonic concentrator with the IMSAR transducer. The IMSAR transducer has an M12x1.75 thread. Therefore, the following data must be entered as parameters (table 8): hole diameter = 10.2 mm, thread diameter = 12 mm, hole depth = 20 mm, thread depth = 15 mm, and the angle for the tip of the hole = 118°.

Table 8

**Parameters for step 4 of the concentrator**

Name	Expression	Value	Description
l1	33.372 [mm]	0.033372 m	upper step length
r1	17.5 [mm]	0.0175 m	upper step radius
l2	35.596 [mm]	0.035596 m	lower step length
r2	10 [mm]	0.01 m	lower step radius
rr	r1 – r2	0.0075 m	radius between steps
modulE	2.1E11	2.1E11	Young's Modulus
alfa	1 [°]	1°	inclination angle
rgaurasc	0.2 [mm]	2E-4 m	wire hole radius
hgaurasc	5 [mm]	0.005 m	wire hole depth
lscula	15 [mm]	0.015 m	electrode length
modulEC u	130 [GPa]	1.3E11 Pa	Young's Modulus for copper
hlipire	3.5 [mm]	0.0035 m	weld height
modulEA g	69 [GPa]	6.9E10 Pa	Young's Modulus for silver
rgaura	5.1 [mm]	0.0051 m	hole radius
hgaura	20 [mm]	0.02 m	hole depth
rfilet	6 [mm]	0.006 m	thread radius
hfilet	15 [mm]	0.015 m	thread depth
beta	59 [°]	59°	angle hole tip

**Complete mesh**

Mesh vertices: 914

Element type: **All elements**

Triangles: 1619

Edge elements: 258

Vertex elements: 19

— Domain element statistics —

Number of elements: 1619

Minimum element quality: 0.5498

Average element quality: 0.8649

Element area ratio: 0.007708

Mesh area: 875.3 mm<sup>2</sup>

Fig. 11. Mesh statistics for step 4 concentrator

The number of elements increased to 1619, and the quality decreased to 0.86 as presented in figure 11.

In figure 12, the addition of the M12x1.75 threaded hole and the stud (material – AISI 4340 steel) led to a decrease in eigenfrequency to a

value of 40921 Hz and a slight increase in amplification to 2.38.

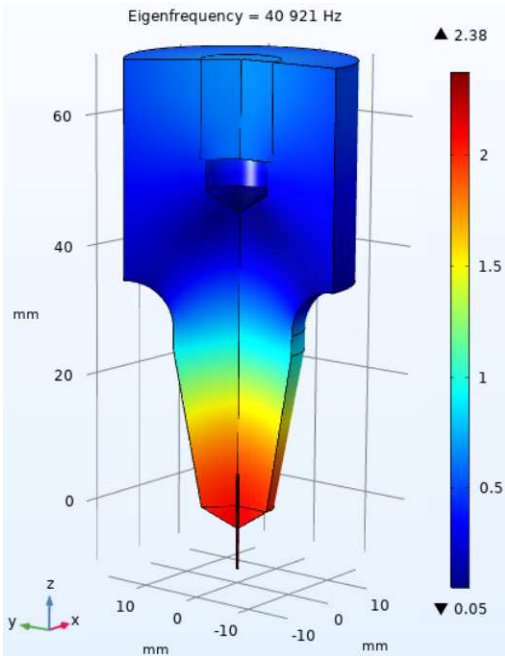


Fig. 12. Eigenfrequency and amplification in step 4 of the concentrator

**Step 5. Introduction of a nodal channel**

A nodal channel is introduced to mark the spot where the concentrator vibrates with minimum amplification.

To determine this position, figure 13 is used, where the amplification limits are modified to isolate the spot where amplification is minimum.

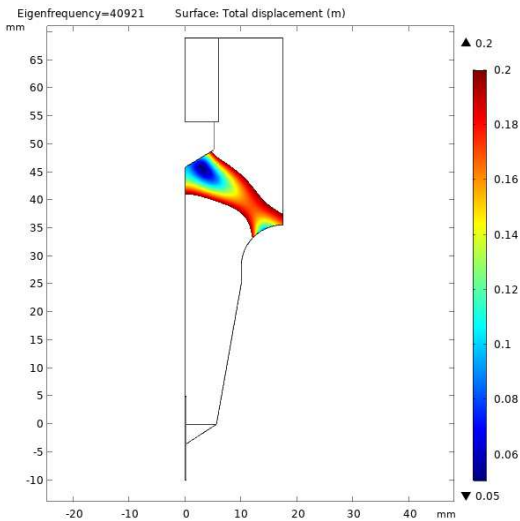


Fig. 13. Nodal channel position determination

The spot is determined to be at a distance of 45.5 mm from the tip of the concentrator,

therefore a channel, used for clamping the US chain by radial screws, is created along the diameter, with a radius of 0.5 mm. Another way of clamping the US chain is through the use of a set of prisms, that makes contact on a small surface around the nodal channel, ensuring that no vibration is passed in the system. The number of elements has increased to 2131, and the quality decreased to 0.8519 as presented in figure 14.

Complete mesh	
Mesh vertices:	1185
Element type:	All elements
Triangles:	2131
Edge elements:	288
Vertex elements:	22
— Domain element statistics —	
Number of elements:	2131
Minimum element quality:	0.5498
Average element quality:	0.8519
Element area ratio:	0.002258
Mesh area:	875 mm <sup>2</sup>

Fig. 14. Mesh statistics for step 5 concentrator

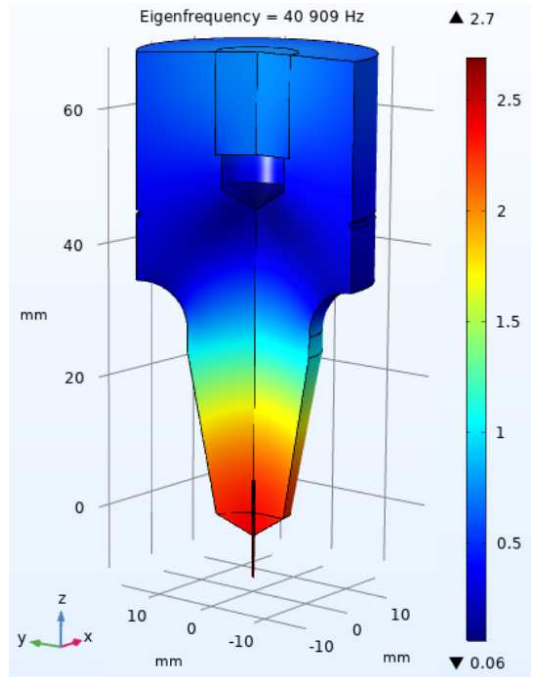


Fig. 15. Eigenfrequency and amplification in step 5 of the concentrator

Figure 15 shows the step 5 concentrator with the nodal channel. Eigenfrequency decreased from 40921 Hz to 40909 Hz, and the amplification increased from 2.38 to 2.7.

**Step 6. Calibration of step lengths**

Since the eigenfrequency of the concentrator  $f_{cr} = 40909$  Hz is over the target eigenfrequency of  $f_{tr} = 40805$  Hz, calibration is done by modifying the upper step length ( $l_1$ ) and lower step length ( $l_2$ ).

Increasing the length of the steps leads to a decrease in eigenfrequency and vice versa.

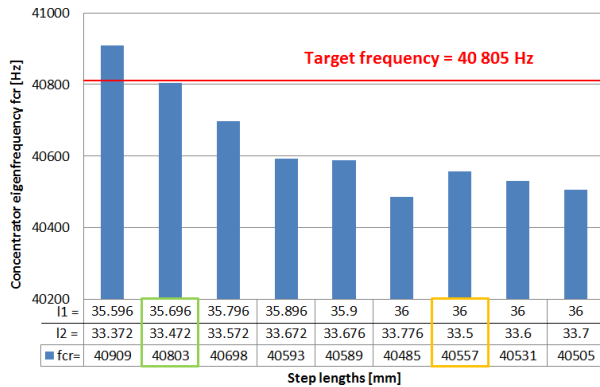
Table 9 illustrates the modifications made to achieve the target eigenfrequency.

Table 9

**Eigenfrequency variation as a function of steps length**

$l_1$ [mm]	$l_2$ [mm]	$f_{cr}$ [Hz]
33.372	35.596	40 909
33.472	35.696	40 803
33.572	35.796	40 698
33.672	35.896	40 593
33.676	35.9	40 589
33.776	36	40 485
33.5	36	40 557
33.6	36	40 531
33.7	36	40 505

Figure 16 provides a graphically overview of the changes in step lengths and the eigenfrequency obtained.



**Fig. 16.** Eigenfrequency as a function of step lengths

The target eigenfrequency is achieved at values of  $l_1 = 33.472$  mm and  $l_2 = 35.696$  mm (green). However, since the concentrator was virtually modelled, these values cannot be chosen as they do not allow adjustments after physical processing.

For this reason, the values of  $l_1 = 33.5$  mm and  $l_2 = 36$  mm (orange) are chosen, which ensure a natural frequency of 40557 Hz and allow physical adjustments (through machining of  $l_1$  – decreasing the length of  $l_1$ ) to reach the target eigenfrequency.

Due to the changes in lengths, the nodal channel was repositioned at a distance of 46.3 mm, without altering the eigenfrequency. The parameters of the final concentrator are presented in table 10.

Table 10

**Parameters for step 6 (final) of the concentrator**

Name	Expression	Value	Description
l1	33.5 [mm]	0.0335 m	upper step length
r1	17.5 [mm]	0.0175 m	upper step radius
l2	36 [mm]	0.036 m	lower step length
r2	10 [mm]	0.01 m	lower step radius
rr	$r1 - r2$	0.0075 m	radius between steps
modulE	2.1E11	2.1E11	Young's Modulus
alfa	1 [°]	1°	inclination angle
rgaurasc	0.2 [mm]	2E-4 m	wire hole radius
hgaurasc	5 [mm]	0.005 m	wire hole depth
lscula	15 [mm]	0.015 m	electrode length
modulECu	130 [GPa]	1.3E11 Pa	Young's Modulus for copper
hlipire	3.5 [mm]	0.0035 m	weld height
modulEA	69 [GPa]	6.9E10 Pa	Young's Modulus for silver
rgaura	5.1 [mm]	0.0051 m	hole radius
hgaura	20 [mm]	0.02 m	hole depth
rfilet	6 [mm]	0.006 m	thread radius
hfilet	15 [mm]	0.015 m	thread depth
beta	59 [°]	59°	angle hole tip
rcanal	0.5 [mm]	0.005 m	channel radius
zcanal	46.3 [mm]	0.0463 m	Z channel position

Figure 17 shows the final concentrator model with an eigenfrequency  $f_{cr} = 40557$  Hz, and an amplification coefficient  $K = 2.71$ .

In Figure 18, it can be observed that the number of elements is 2137, and the quality factor remains constant at 0.85.

The concentrator will undergo successive testing and machining to reach the target frequency of 40805 Hz.

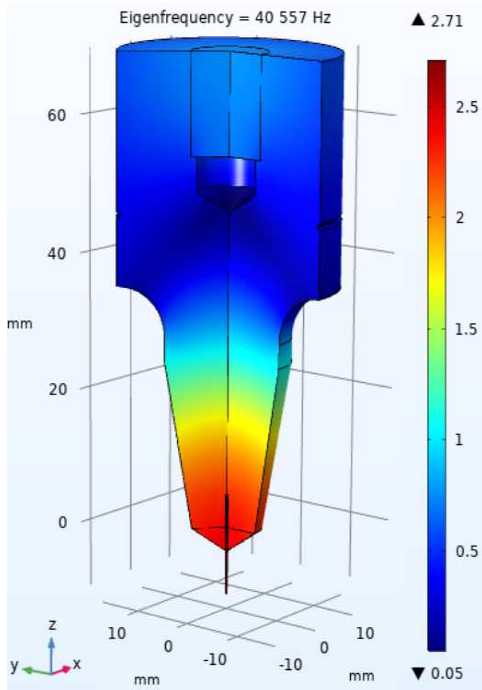


Fig. 17. Eigenfrequency and amplification in step 6 (final) of the concentrator

Complete mesh	
Mesh vertices:	1189
Element type:	All elements
Triangles:	2137
Edge elements:	290
Vertex elements:	22
— Domain element statistics	
Number of elements:	2137
Minimum element quality:	0.5498
Average element quality:	0.8551
Element area ratio:	0.001887
Mesh area:	881.2 mm <sup>2</sup>

Fig. 18. Discretization characteristics for step 6 (final) of the concentrator

An overview of all steps followed is presented in table 11:

Table 11

Overview of concentrator changes per step				
Step	f <sub>cr</sub> [Hz]	K [-]	Mesh quality	Number of elements
initial	36 078	2.96	0.9256	1 331
1	36 598	3.03	0.9138	1 332
2	42 202	3.34	0.9119	1 278
3	41 425	2.37	0.8747	1 565
4	40 921	2.38	0.8649	1 619
5	40 909	2.7	0.8519	2 131
6	40 557	2.71	0.8551	2 137

The final model of the concentrator is then imported into Solidworks 2016 and introduced into the feed system assembly.

For the assembly of the concentrator with the IMSAR transducer, an 18 mm long M12x1.75 stud (figure 19) is used, made of the same material as the concentrator – AISI 4340 steel.

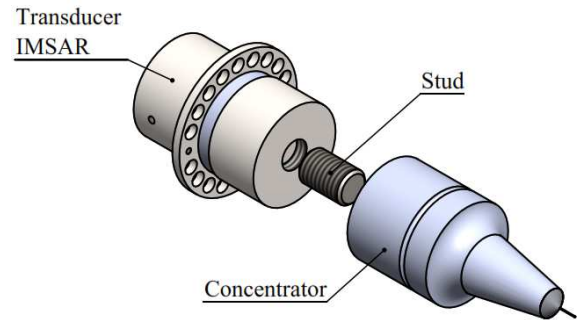


Fig. 19. Ultrasonic chain assembly

## 5. TESTING

To verify the validity of the 3D model and the achieved eigenfrequency of the designed ultrasonic concentrator, a test was conducted. The ultrasonic chain was connected to a digital oscilloscope as well as a variable frequency tone generator (as seen in figure 20).

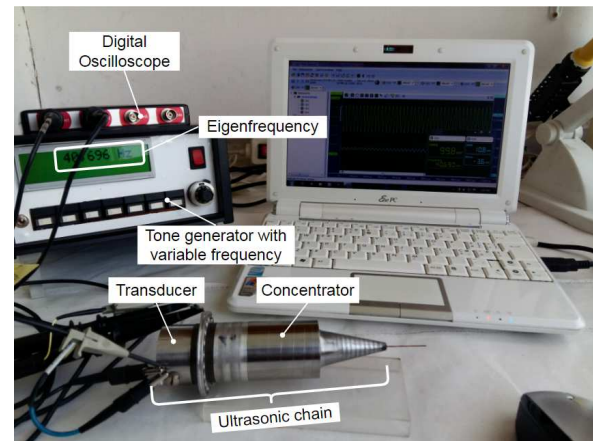


Fig. 20. Experimental stand and eigenfrequency

The simplified electric scheme used for the experimental stand is presented in figure 21.

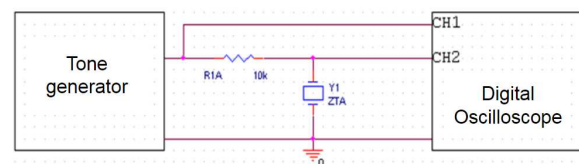
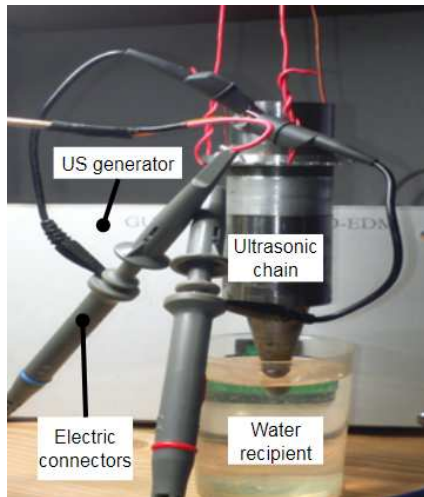


Fig. 21. Experimental scheme of the experimental stand

The eigenfrequency achieved during testing was 40696 Hz.

In order to observe the ultrasonically cavitation phenomena, the tip of the ultrasonic horn, was immersed in a water recipient, with the ultrasonic chain connected to the ultrasonic generator that was set to the resonance frequency of 40696 Hz, as seen in figure 22.



**Fig. 22.** Testing of ultrasonically induced cavitation

Additional machining of the upper step length (by cutting) of the concentrator was executed, together with subsequent tests to achieve the targeted eigenfrequency of 40805 Hz.

If the eigenfrequency of the ultrasonic concentrator must be lowered, material needs to be added on the concentrator, by additive technologies. However, this addition would significantly escalate costs and, as a result, is generally avoided.

It's important to target a lower eigenfrequency in the simulation – to allow for appropriate adjustments, and avoid additive technologies, thus having significantly lower costs.

## 6. RESULTS AND DISCUSSION

The conducted test verified the actual eigenfrequency of the designed ultrasonic concentrator. The achieved frequency of 40696 Hz indicates substantial progress towards the desired target of 40805 Hz. However, further adjustments through machining of the concentrator will be made to reach the targeted eigenfrequency by slightly reducing the step lengths.

## 7. CONCLUSIONS

The modelling approach presented in this study offers a method for the design and optimization of ultrasonic concentrators tailored to specific eigenfrequency applications. By utilizing Comsol Multiphysics software with the Structural Mechanics module and the Eigenfrequency study, the concentrator's geometry and parameters were systematically adjusted to achieve the targeted eigenfrequency of ultrasonic transducer, which is the resonance frequency of 40805 Hz.

Through incremental adjustments the concentrator's eigenfrequency was fine-tuned. Each step resulted in geometry changes as well as changes to the number of elements, quality factor, eigenfrequency and amplification coefficient.

The concentrator modelling emphasized that some geometrical parameters determine the increase of eigenfrequency like, step lengths, inclination angle, which also grows the amplification coefficient. The addition of Ag welding of tool electrode lowers the own frequency, but the filiform electrode has no significant influence on the target frequency.

The final concentrator design, with an eigenfrequency of 40557 Hz and an amplification coefficient of 2.71, showcases the effectiveness of the modeling approach.

However, it is important to note that the physical adjustments through machining are absolutely necessary to precisely achieve the resonance frequency of 40805 Hz. The real natural frequency of the ultrasonic concentrator with integrated tool- electrode is inevitable affected mainly by factual materials characteristics, with direct influence of ultrasonic waves propagation. The testing conducted provides tangible evidence of the numerical modeling and optimization approach's effectiveness in approximating the desired frequency. This verification underscores the reliability of designing ultrasonic concentrators optimized for certain eigenfrequencies.

## 8. FURTHER RESEARCH

Potential areas for further research include:

- a. Conduct experimental investigations of the influence of the inclination angle on the concentrator's eigenfrequency, as well as methods to make the concentrator lighter and to require fewer machining operations.
- b. Explore technological methods to recover concentrators that exceeded the target eigenfrequency, as well as low-cost prevention methods.
- c. Investigate methods to fine-tune machining of concentrator in adjustment phase. Precision is crucial in achieving the desired eigenfrequency. By optimizing machining processes and parameters, as well as the tools used, the potential for exceeding the target eigenfrequency can be minimized, leading to more predictable and reliable results.
- d. Compare the performance of the optimized concentrator with other existing concentrator designs, such as horn-type concentrators, to evaluate its advantages and limitations.
- e. Conduct more physical experiments to validate the performance of the optimized concentrator in a real microEDM+US technological system, under conditions of real machining. Compare experimental results with numerical simulations to verify the accuracy of the numerical model and optimization process. These directions can provide practical insights that can be directly applied in designing and optimizing concentrators for specific eigenfrequencies.

## 9. ACKNOWLEDGEMENTS

The testing of the ultrasonic chain was achieved on the experimental stand and ultrasonic generator constructed by Engineer N. Stefan.

## 10. REFERENCES

- [1] Sami, C., Luc, L., Gunther, R., Tullio, T., *CIRP Encyclopedia of Production Engineering*, 2nd edition, Springer, ISBN: 3662531194 Paris, France, 2019.
- [2] Makenzi, M. M., Ikua, B. W. Ikua., *A review of flushing techniques used in electrical discharge machining*, Proceedings of 2012 Mechanical Engineering Conference on Sustainable Research and Innovation, Vol. 4, pp. 162 - 165, 2012.
- [3] Liu, Q., Zhang, Q., Zhang, M., Zhang, J., *Review of Size Effects in Micro Electrical Discharge Machining*, Precision Engineering, Vol. 44, pp. 29 - 40, 2016.
- [4] Davim, J. P., *Nontraditional Machining Processes: Research Advances*, Springer, Aveiro, Portugal, ISBN: 144715178X, 2013.
- [5] Hourman, M., Sarhan, A. A., Sayuti, M., *Micro-electrode fabrication processes for micro-EDM drilling and milling: a state-of-the-art review*, The International Journal of Advanced Manufacturing Technology, Vol. 91, pp. 1023 - 1056, 2017.
- [6] Ghiculescu, D., Marinescu, N.I., Jitianu, G., *On precision improvement by ultrasonics-aided electrodischarge machining*, Estonian Journal of Engineering, Vol. 15, pp. 24 - 33, 2009.
- [7] Hou, S., Bai, J., *A novel ultrasonic vibration-assisted micro-EDM method to improve debris removal performance using relative three-dimensional ultrasonic vibration (RTDUV)*, The International Journal of Advanced Manufacturing Technology, Vol. 127, pp. 5711-5727, 2023.
- [8] Wang, P., Yu, D., Li, M., *A study on ultrasonic-assisted micro-EDM of titanium alloy*, The International Journal of Advanced Manufacturing Technology, Vol. 121, pp. 2815-2829, 2022.
- [9] Raza, S., Nadda, R., Nirala, C. K., *Sensors-based discharge data acquisition and response measurement in ultrasonic assisted micro-EDM drilling*, Measurement: Sensors, Vol. 29, 2023.
- [10] Li, Z., Tang, J., Bai, J. *A novel micro-EDM method to improve microhole machining performances using ultrasonic circular vibration (UCV) electrode*, International Journal of Mechanical Sciences, Vol. 175, 2020.
- [11] Singh P., Yadava, V., Narayan, A., *Performance Study of Ultrasonic-*

*Assisted Micro-Electrical Discharge Machining of Inconel 718 Superalloy Using Rotary Tool Electrode*, Journal of The Institution of Engineers(India): Series C, Vol. 104, pp. 149 – 162, 2023

[12] Astashev, V. K., Babitsky, V. I., *Ultrasonic processes and machines: dynamics, control and applications*, Springer, ISBN: 978-3-540-72061-4, 2007.

## MODELAREA ȘI SIMULAREA UNUI CONCENTRATOR ULTRASONIC UTILIZAT ÎN CADRUL UNUI SISTEM DE AVANS PENTRU MICROELECTROEROZIUNE ASISTATĂ DE ULTRASUNETE

**Rezumat:** Această lucrare prezintă o abordare de modelare numerică pentru optimizarea unui concentrator ultrasonic, în aplicații de microelectroeroziune (microEDM), la o frecvență țintă de 40805 Hz. Dimensiunile și forma concentratorului sunt ajustate printr-un proces de optimizare pentru a obține un coeficient de amplificare ridicat. Un canal nodal este utilizat pentru a marca regiunea, de pe concentrator, unde amplificarea este minimă. Concentratorul rezultat are o frecvență proprie de 40557 Hz și un coeficient de amplificare de 2.71. Concentratorul și transductorul sunt conectate folosind un șurub M12 cu lungimea de 18 mm. Testarea validează modelul, rezultând o frecvență proprie de 40696 Hz, care este ulterior prelucrată pentru a atinge frecvența țintă. Studiul reprezintă o metodă de proiectare și optimizare a concentratorilor la frecvențe specifice.

**Cuvinte cheie:** microelectroeroziune, concentrator ultrasonic, sistem de avans, transductor, frecvență proprie.

**Bogdan-Ionut CRISTEA**, PhD Student, National University of Science and Technology “Politehnica” of Bucharest, Department of Manufacturing Engineering, [cristea.ibogdan@gmail.com](mailto:cristea.ibogdan@gmail.com).

**Liviu Daniel GHICULESCU**, Prof. Habil. PhD, Eng., National University of Science and Technology “Politehnica” of Bucharest, Department of Manufacturing Engineering, [daniel.ghiculescu@upb.ro](mailto:daniel.ghiculescu@upb.ro).

**Aurel Mihail TITU**, Prof. Habil. PhD, Eng. PhD. Ec., University “Lucian Blaga” of Sibiu, Industrial Engineering and Management Department, [mihail.titu@yahoo.com](mailto:mihail.titu@yahoo.com).

**Constantin-Cristian DEOPALE**, PhD Student, National University of Science and Technology “Politehnica” of Bucharest, Department of Manufacturing Engineering, [cristian.deopale@outlook.com](mailto:cristian.deopale@outlook.com).